Article

Application of Fractional Order-PID Control Scheme in Automatic Generation Control of a Deregulated Power System in the Presence of SMES Unit

Nagendra Kumar [1], Majed A. Alotaibi [2,*], Akhilesh Singh [3], Hasmat Malik [4,*] and Mohammed E. Nassar [5]

1 Electrical & Electronics Engineering Department, G. L. Bajaj Institute of Technology & Management, Greater Noida 201306, India; nagendra.kumar@glbitm.ac.in
2 Department of Electrical Engineering, College of Engineering, King Saud University, Riyadh 11421, Saudi Arabia
3 Electrical and Electronics Engineering Department, Nanhi Pari Institute of Technology, Pithoragarh 262501, India; akhil09msingh@gmail.com
4 BEARS, University Town, NUS Campus, Singapore 138602, Singapore
5 Department of Electrical and Computer Engineering, University of Waterloo, Waterloo, ON N2L 3G1, Canada; mnassar@uwaterloo.ca
* Correspondence: majedalotaibi@ksu.edu.sa (M.A.A.); hasmat.malik@gmail.com (H.M.)

Abstract: A fractional order PID (FOPID) control technique for automatic generation control (AGC) in a multi-area power system is presented in this study. To create a reliable controller, a variety of control strategies were used. The load frequency control (LFC) problem in a power system implementing different power transactions, such as bilateral and Poolco transactions, are investigated here. Because any control scheme's performance is only as good as its parameters, the parameters of the designed control scheme were determined using the big bang big crunch (BBBC) algorithm. Furthermore, in this work, the effect of a superconductive magnetic energy storage (SMES) unit is addressed in the given test (two and four area) systems. When confronted with a fluctuation in immediate load, the SMES unit is thought to follow the initial drop in frequency and tie-line power in order to increase LFC. It is evident that the performance of an FOPID control scheme is improved in the presence of an SMES unit and it provides frequency, tie-line power, change in generation with reduced oscillations and settling time.

Keywords: BBBC; deregulation; FOPID; LFC; power system; SMES

1. Introduction

Load frequency control (LFC) is a mechanism that divides the load between generators and maintains a generally consistent frequency in an electric power system. The power system is a massive, complex technical system with multiple control zones. Tie-lines connect each control region to the next. As a result, maintaining the system's balance is a challenging task. Any interruption or change in load can cause a shift in system frequency and tie-line power, which may have severe effects such as the stalling of generators, etc., if not addressed properly [1].

The electrical sector's structure, working conditions and control parameters have all changed since deregulation was implemented. LFC's responsibilities have also increased as a result of this.

A detailed description of the restructuring LFC, including issues, modifications and changes, is presented in [2].

An optimal controller is termed as the heart of the LFC scheme. In the literature, several approaches, starting from classical to modern, as well as optimization-based, have been presented regarding designing an optimal controller [3]. For a very long time, controllers such as PID (proportional integral derivative) have been preferred among researchers due to their simple and convenient implementation [4]. LFC/AGC is a key factor in designing

an electric power system with optimal considerations and aspects of quality and reliability in the electric power supply.

A sudden load perturbation leads to electromechanical oscillations. Therefore, a fast-acting energy storage technology, i.e., SMES, battery and pump storage, is needed to offer fast response and minimum vibrations. A mismatch can lead to a complete system failure; therefore, a steady, fast and supremely correct controller design is ruled for constant desired frequency. It is reported that SMES improves load dynamics, controls real and reactive power, and is therefore widely used as an oscillation stabilizer in LFC problems [5,6]. The optimal installation of the number of SMES units was explained in [5], which states that it is not necessary to install an SMES unit in each control area. A single SMES unit can be used to control the frequency of other regions too, which works effectively [6].

Researchers are increasingly working on fractional order (FO) control schemes as an alternative to traditional control approaches. An FOPID control scheme is termed as an extension of PID and is used in a variety of fields such as design [7], stabilization [8] and automatic voltage controller (AVR) [9]. Various optimization approaches have been successfully implemented to obtain the parameters of FOPID parameters [10–12].

A good control approach must have optimal parameters in order to have optimal performance. There are several other algorithms particle swarm optimization (PSO), genetic algorithm (GA), imperialistic competition algorithm (ICA), harmony search (HS), are available in the literature. The authors used BBBC [13] to identify the best parameters of an FOPID controller, after comparing it to other search algorithms such as ICA and GA [14–20].

The power flow between control areas is regulated by load frequency control to keep the frequency constant. However, as a result of deregulation, a variety of power transactions have formed in the electrical sector, affecting power transfer between areas. Through the Disco participation matrix, any Disco can now have power contracts with Gencos of the same and other areas via bilateral transactions. Another type of power contract is the Poolco transaction.

Two and four area power systems were chosen as test systems to assess the performance of the designed control scheme. The designed control scheme was evaluated in terms of settling time, oscillations and other time-domain responses using a range of load disturbances and both (Poolco plus bilateral) power transactions. A comparison reveals that at steady state, the targeted parameters are settling to their desired levels.

Different simulation results were obtained using the FOPID controller at MATLAB/Simulink platform. It is observed that the FOPID controller gives increased performance with an SMES unit. It also establishes that the settling time of various responses is reduced significantly using the SMES unit.

Novelty: The use of FOPID-SMES control scheme for load frequency control of two and four-area power systems is provided in this paper. This study contributes by offering a complete performance investigation of a designed control scheme employing actual test system.

The main highlights of this paper are:

(1) Two area thermal and four area hydro-thermal power systems are taken for the case study, and a simulation model of the two and four area power systems is modeled.
(2) An FOPID control scheme modelled using BBBC is implemented.
(3) The performance and effectiveness of the designed control scheme are checked under different disturbance scenarios, with and without an SMES device.
(4) It is observed that, in all cases, FOPID with SMES performs better, specifically in terms of settling time and oscillation.

Figure 1 represents a graphical summary of the research presented in this study. The rest of the article is structured as follows: Section 2 introduces the modelling of test systems. The designed approach is presented in Section 3. The results and conclusion are discussed in Sections 4 and 5.
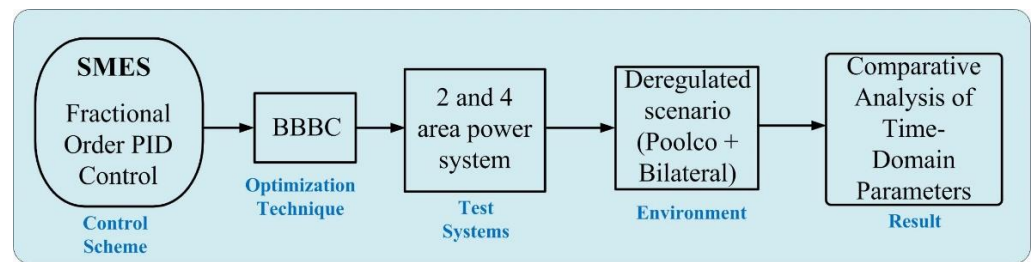
Figure 1. Graphical summary.

2. Modelling of Multiarea Power System in Deregulated Environment

Many traditional power system improvements occurred as a result of deregulation, and such a scenario becomes increasingly crucial in order to manage frequency control. In today environment, Disco (distribution company) has the option of selecting a power contract from a Genco (generation company) in their jurisdiction or forming their own. Bilateral trade is a method of power transmission that is implemented via DPM. The area control error is eliminated with the help of a controller and given by Equation (1).

$$ACE_i = B_i \Delta F_i + \Delta Ptie_i \tag{1}$$

Transactions such as Poolco and bilateral are used for electricity transmission in a deregulated system. Equation (2) shows the impact of bilateral trades on tie-line.

$$\Delta Ptie_{i-new} = \Delta Ptie_i + \sum_{\substack{j=1 \\ i \neq j}}^{n} D_{ij} - \sum_{\substack{j=1 \\ i \neq j}}^{n} D_{ji} \tag{2}$$

where n is total areas, D_{ij}/D_{ji} shows Discos' demands to Gencos, and $\Delta Ptie_i$ is tie-line power deviation. This variation in tie-line modifies the earlier ACE as presented using Equation (3).

$$ACE_i = B_i \Delta F_i + \Delta Ptie_{i-new} \tag{3}$$

Finally, the net generation of different Gencos is evaluated by Equation (4).

$$\Delta P_{gi} = \sum_j cpf_{i_j} \Delta P_{Dj} \tag{4}$$

where P_D is the total load demand.

SMES and Its Control Strategy

Figures 2 and 3 show an SMES unit and its control structure [7]. The detailed literature regarding SMES can be referred from [7,8]. The expression of DC voltage of an SMES unit can be written as

$$E_L = 2V_{d0} \cos \alpha_c - 2I_L R_{cm} \tag{5}$$

where E_L = DC voltage across the coil (kV), V_{d0} = maximum circuit bridge voltage (kV), R_{cm} = equivalent commutating resistance (Ω), I_L = current through coil (kA) and α_c is the firing angle (degrees). For an ith area, the expression for DC voltage is given in Equation (6)

$$\Delta E_{L\_i}(s) = \left[\frac{K_{SMES}}{1 + T_{dc\_con\_i}} \right] \Delta Error \tag{6}$$

where ΔE_L = Change in converter voltage, T_{dc_con} = time delay (s), K_{SMES} = control loop gain and $\Delta Error$ = ACE.

The ACE signal is defined in Equation (3). On placing the value of ACE from Equation (3) in Equation (6), convertor voltage can be modified as

$$\Delta E_{L\_i}(s) = \left[\frac{K_{SMES}}{1 + T_{dc\_con\_i}}\right][B_i\Delta f_i + \Delta Ptie_{i-error}] \tag{7}$$

To respond to a load disturbance, the SMES control loop uses coil current deviation (ΔI_L) as a feedback to provide the quick restoration. Therefore, Equation (7) can be modified as

$$\Delta E_{L\_i}(s) = \left[\frac{K_{SMES}}{1 + T_{dc\_con\_i}}\right][(B_i\Delta f_i + \Delta Ptie_{i-error}) - K_{IL}\Delta I_{L\_i}] \tag{8}$$

where K_{IL} = Coil current deviation feedback loop gain (kV/kA).

The deregulated LFC scheme with different transactions, incorporation of an SMES unit and a load deviation is shown in Figure 4.
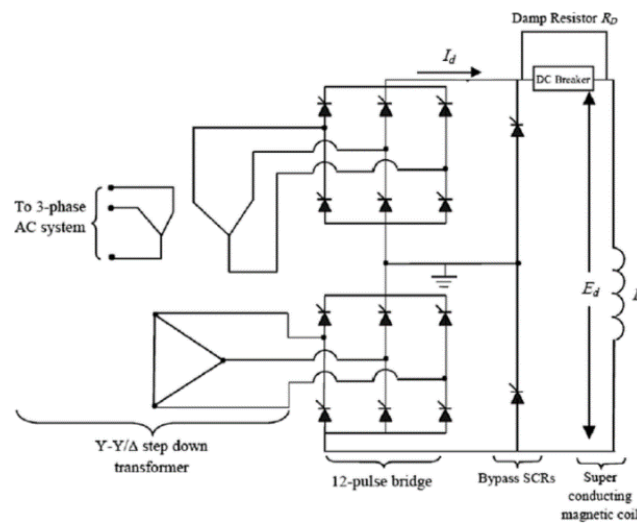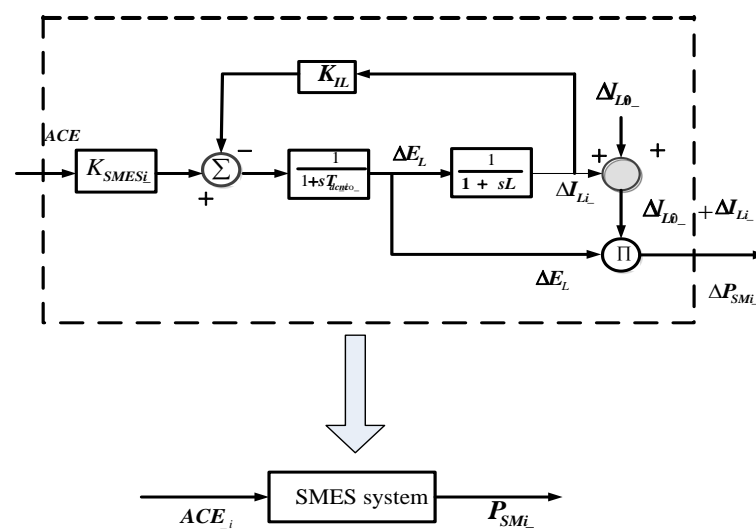
Figure 2. SMES Unit.
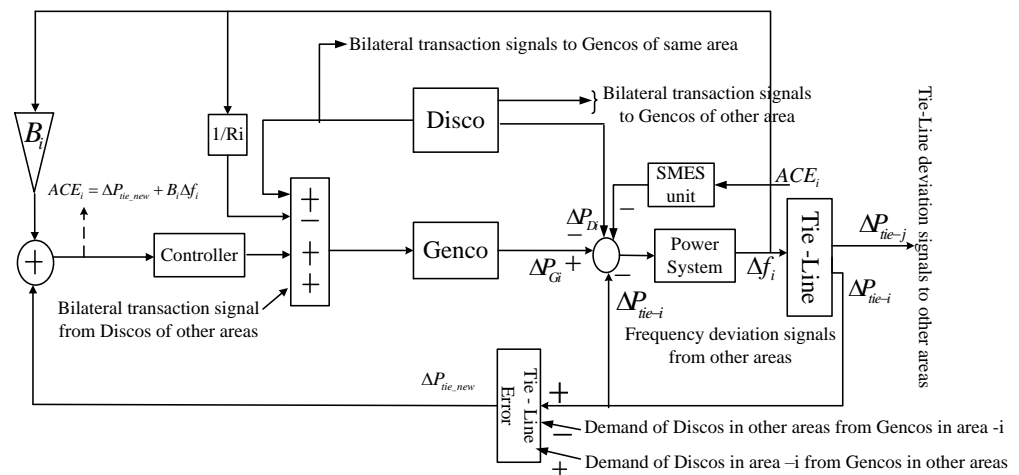
Figure 3. SMES Control Scheme.

Figure 4. Block Diagram of LFC scheme with SMES Unit.

3. FOPID Control Scheme Using BBBC

For a successful LFC, a good control scheme is required. Researchers have devised a variety of control systems, but the fractional-order control scheme is presently in use because it has advantages over traditional control schemes in terms of reduced steady-state error, less oscillation and shortened settling time. The most frequent structure of a FOPID control scheme is shown in Figure 5.
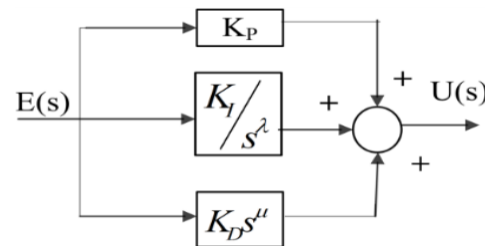

Figure 5. FOPID Structure.

where

$$u(t) = K_P e_r(t) + K_I D^{-\lambda} e_r(t) + K_D D^{\mu} e_r(t) \tag{9}$$

The Laplace form of Equation (9) is given in Equation (10).

$$G_{FOPID}(s) = K_P + K_I s^{-\lambda} + K_D s^{\mu} \tag{10}$$

where K_P, K_I, and K_D = FOPID parameters and λ/μ is fractional integrator/differentiator.

Equation (11) gives the fitness function, which is used to design the FOPID control scheme.

$$F = \frac{1}{n} \sum_{i=1}^{n} \left[(ACE_i)^2 \right] \tag{11}$$

- Steps to design FOPID using BBBC

  Step 1. The population of parameters is generated in this step.

$$x_{ij}{}^{(k)} = x_{i(min)}{}^{(k)} + rand.(x_{i(max)}{}^{(k)} - x_{i(min)}{}^{(k)}) \tag{12}$$

where x = FOPID parameters, k = total number of areas, i = total parameters, and j = total population size.

Step 2. The fitness function (11) is assessed for the population created in step 1 in this phase.

Step 3. This phase entails constructing the center of mass as shown in Equation (13).

$$X_{com} = \frac{\sum\limits_{j=1}^{P} \frac{x_{ij}^{(k)}}{F_j}}{\sum\limits_{j=1}^{P} \frac{1}{F_j}} \tag{13}$$

Step 4. A new population is produced near the center of mass in this step.

$$x_{ij(new)}^{k} = X_{com} + \frac{r.\alpha(x_{i(max)}^{k} - x_{i(min)}^{k})}{K} \tag{14}$$

where α = parameter limit the size, K = iteration number, r = random number.

Step 5. The following best parameters are generated in this step.

$$x_{ij}^{k}{}_{(next)} = min\left\{ F(x_{ij}^{k}{}_{(previous)}),\ F(x_{ij}^{k}{}_{(new)}) \right\} \tag{15}$$

Step 6. The best fitness function and its related parameters are determined in this step. Figure 6 shows the flowchart of the BBBC algorithm.
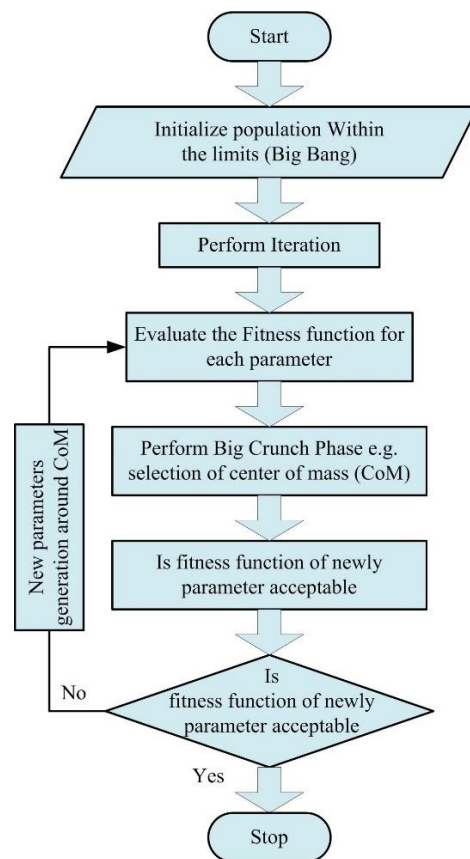

Figure 6. General flowchart of BBBC algorithm.

4. Results and Discussion

The simulation was performed using the MATLAB Simulink platform. The Simulink models of both tests were modeled to discuss the LFC scheme with Poolco and Bilateral transactions. It is observed that system responses, i.e., frequency/tie-line power disturbed after a load perturbation. SMES has a role in reducing disturbances to a safe limit. After the SMES, common control elements take over to adjust the deviation.

4.1. Two-Area System (Bilateral + Poolco Transactions)

In this section, the performance of the FOPID control scheme in two area power systems (with and without an SMES unit) is discussed. The LFC scheme for two area systems is developed on the basis of Figure 4. Non-reheat turbine units are taken in both area cases. In every area, 2-Gencos and 2-Discos are considered. The developed controller is examined in every area when load disturbances of 0.2 pu is applied. It is considered that the SMES unit is presumed only in area-1 and engages in every Genco LFC scheme. It is assumed that Gencos have fixed participation factors, which are given as

$$\left. \begin{array}{l} \mathrm{pf}_1 = 0 \ \text{for Genco1} \\ \mathrm{pf}_2 = 1 \ \text{for Genco2} \end{array} \right\} \text{area} - 1 \ \text{and} \ \left. \begin{array}{l} \mathrm{pf}_3 = 0.5 \ \text{for Genco3} \\ \mathrm{pf}_4 = 0.5 \ \text{for Genco4} \end{array} \right\} \text{area} - 2$$

A given DPM is used for bilateral transactions.

$$\mathrm{DPM} = \begin{array}{c} \\ \mathrm{G1} \\ \mathrm{G2} \\ \mathrm{G3} \\ \mathrm{G4} \end{array} \begin{array}{cccc} \mathrm{D1} & \mathrm{D2} & \mathrm{D3} & \mathrm{D4} \\ \left[\begin{array}{cccc} 0.3 & 0.25 & 0 & 0.3 \\ 0.2 & 0.2 & 0 & 0 \\ 0 & 0.25 & 1 & 0.7 \\ 0.3 & 0.25 & 0 & 0 \end{array} \right] \end{array}$$

A load of 0.2 pu is employed to check the effectiveness of the designed control scheme. The responses of both areas' frequency were disturbed after this load perturbation. To bring back these frequencies to their desired values, LFC makes a change in Genco generation and restores frequencies of both areas to their scheduled values. The SMES unit takes care of the initial dampening in the frequency deviation response. The variation in frequencies is substantially more significant in magnitude in the absence of the SMES unit, as seen in Figure 7. The frequency variations in area-1 and area-2 abruptly vanish, resulting in reduced oscillation when the SMES system is used.
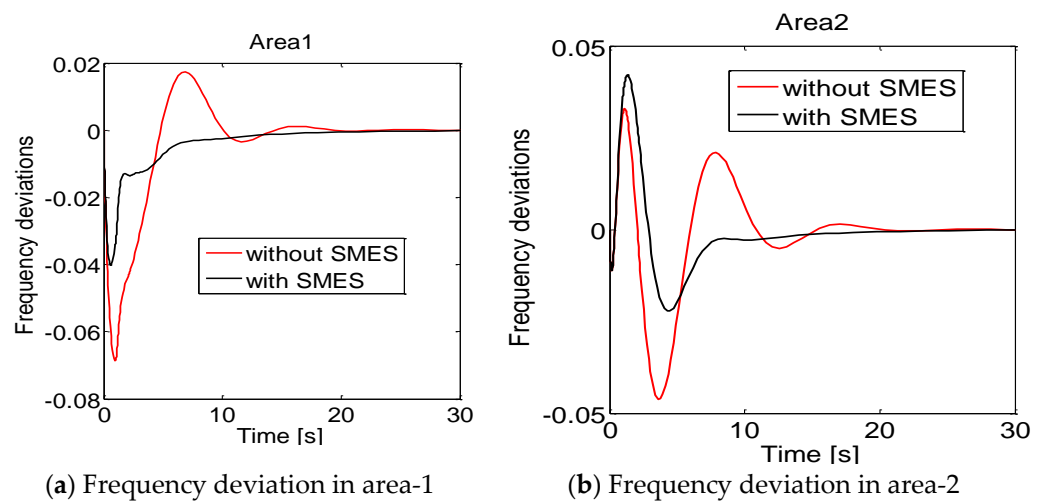

(**a**) Frequency deviation in area-1   (**b**) Frequency deviation in area-2

Figure 7. Frequency settlement in both areas (rad/s).

In order to compensate for these deviations in frequency, the Gencos of each area regulate their generation as per Equation (4), which can be written as

$$(\Delta P_{Gi})_{bi} = cpf_{i1}\Delta P_{L_1} + cpf_{i2}\Delta P_{L_2} + cpf_{i3}\Delta P_{L_3} + cpf_{i4}\Delta P_{L_4}$$
$$\text{for } i = 1, 2, 3, 4$$

This can further be written as

$$(\Delta P_{G1})_{bi} = 0.3 \times 0.1 + 0.25 \times 0.1 + 0 \times 0.1 + 0.3 \times 0.1 = 0.085 \ \text{pu}$$

$$(\Delta P_{G2})_{bi} = 0.2 \times 0.1 + 0.2 \times 0.1 + 0 \times 0.1 + 0 \times 0.1 = 0.04$$

It is observed that after the settlement of bilateral contracts, a power requirement of 0.025 pu is still needed. This is where participation factors of Gencos come into the picture. This additional power is supplied by the Gencos as per their participation factors and can be represented as

$$(\Delta P_{G(area-1)})_{net} = (0.085)_{bi} + (0)_{pf} = 0.085 \text{ pu}$$

$$(\Delta P_{G\ (area-1)})_{net} = (0.04)_{bi} + (0.025)_{pf} = 0.065 \text{ pu}$$

The net generation change in Gencos of area-1 is depicted in Figure 8. It is clear that Gencos are settling to their generation as per the requirement.
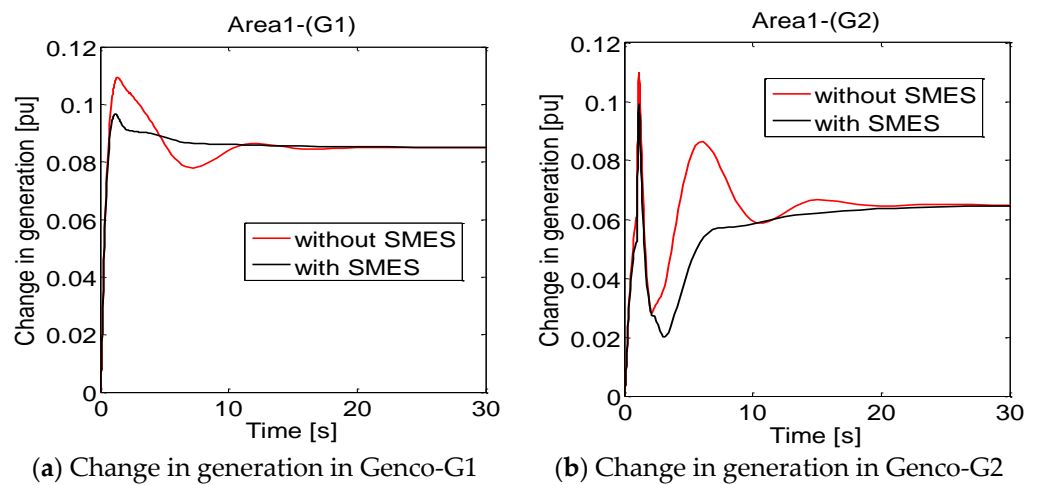

(**a**) Change in generation in Genco-G1   (**b**) Change in generation in Genco-G2

Figure 8. Change in Gencos in area-1 (pu).

Area-2: as it is seen from DPM, G3 has bilateral contracts with Discos of both areas; therefore, in order to bring the frequency back, G3 changes its generation to supply 0.025 pu to D2 (area-1), 0.1 pu to D3 (area-2) and 0.07 pu to D4 (area-2). G4 of area-2 has bilateral contracts with Discos of area-1 only. It changes its output to supply 0.03 pu to D1 (area-1) and 0.025 pu to D2 (area-1).

The total output of Gencos of area-2 is given in Figure 9.

$$(\Delta P_{G(area-2)})_{net} = 0 \times 0.1 + 0.25 \times 0.1 + 1 \times 0.1 + 0.7 \times 0.1 = 0.195$$

$$(\Delta P_{G(area-2)})_{net} = 0.3 \times 0.1 + 0.25 \times 0.1 + 0 \times 0.1 + 0 \times 0.1 = 0.055$$

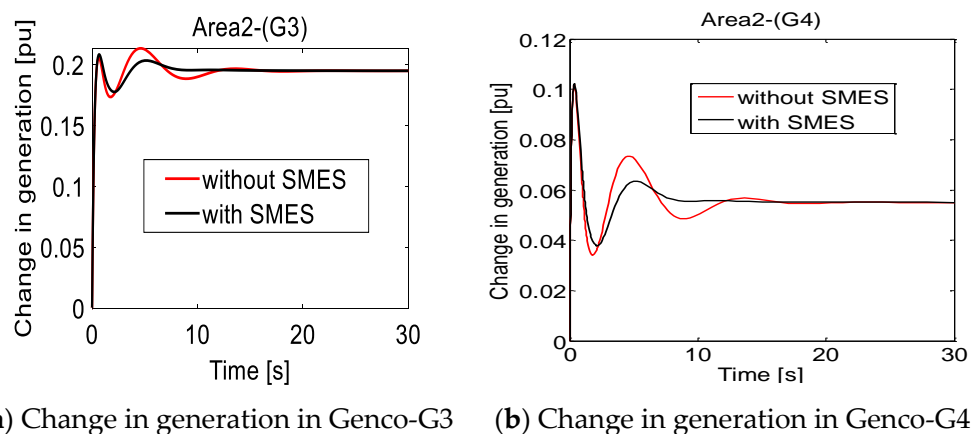(**a**) Change in generation in Genco-G3   (**b**) Change in generation in Genco-G4

Figure 9. Change in Gencos in area-2 (pu).

Equation (16) shows the change in tie-line power, which has a dependency on bilateral transactions. It is evident that load perturbation also affects net power. Due to the effect of bilateral transactions, power is settled to -0.05 pu, given in Figure 10.

$$\Delta Ptie_{i-new} = \sum_{i=1}^{2} \sum_{j=3}^{4} cpf_{ij} \Delta PL_j - \sum_{i=3}^{4} \sum_{j=1}^{2} cpf_{ij} \Delta PL_j = -0.05 \text{ pu} \tag{16}$$
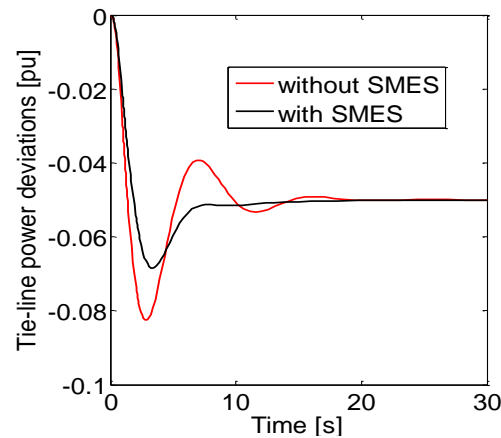

Figure 10. Change in tie-line power flow (pu).

From the above analysis, one can easily verify that FOPID with SMES results in better performance than FOPID without SMES. Table 1 shows a comparison of the performance, and demonstrates that the FOPID controller with an SMES unit provides better dynamic response.

Table 1. Settling time (s) for frequency deviations: (two-area system).

Controller	Settling Time (s)		Overshoots		Undershoots	
	Δf_1	Δf_2	Δf_1	Δf_2	Δf_1	Δf_2
SMES	28	30	0.0	0.04	-0.04	-0.021
No SMES	35	32	0.0175	0.03	-0.0685	-0.045

4.2. Four-Area System (Bilateral + Poolco Power Transactions)

A 75-bus Indian power system given in Table 2 is also considered to check the proposed control scheme. To implement the Poolco transaction, participant factors of Gencos (Table 3) and Discos (Table 4) in all four-areas are chosen on the basis of a bidding process, which includes price and capacity.

Table 2. Control areas—(Four-area power system).

Area	Rating (MW)	Gencos and Discos
Area-1	460	3 Gencos, 3 Discos
Area-2	994	4 Gencos, 3 Discos
Area-3	400	2 Gencos, 3 Discos
Area-4	4470	5 Gencos, 3 Discos

Table 3. Participation Factors—Discos.

Area	Area-1	Area-2	Area-4
Discos	D1	D6	D11
Participation factor	0.2222	0.1429	0.1429

Table 4. Participation factors—Gencos.

Area	Area-1			Area-2	
Gencos	**G1**	**G2**	**G6**	**G8**	
Participation factor	0.6667	0.1111	0.1429	0.7143	
Area		Area-3		Area-4	
Gencos	G9	G10	G11	G13	G15
Participation factor	0.3	0.7	0.3571	0.1429	0.3571

A load change of 50 MW each (area-1 to area-3), and 100 MW (area-4) is employed to simulate evaluated results of FOPID with/without an SMES unit. Following bilateral transactions are taken in different areas.

- Genco G5 (area-2) has a bilateral contract with area-1 and area-4 to provide 10% load of both areas.
- G12 (area-4) has a bilateral contract to provide 20% of area-4 load.
- G11 (area-4) provides 20% load of area-2, while 10% load of area-2 is followed by G4 itself (area-2).

Additional power is needed in different areas when bilateral contracts of different areas are considered as follows: Area-1/45 MW, Area-2/35 MW and Area-4/70 MW. In order to achieve the demand, Poolco transactions are utilized by the ISO.

In area-1: There is a total load demand of 50 MW. In order to meet this load demand, Gencos with bilateral and Poolco contracts with area-1 begin regulating their generation. Genco G1 changes to 30 MW (0.6667 * 45) to response to this load demand, as it has a participation factor of 0.6667. Because it has a participation factor of 0.111; (0.111 * 45), Genco G2 regulates its output by 5 MW. Because of its participation factor of 0.2222, Disco D1 reduces its load by 10 MW ((0.2222 * 45). The remaining 5 MW of load demand is met by Genco G5 of area-2, which has a bilateral contract with area-1 for 10% of total load demand. As a result, Gencos G1, G2 and Disco D1 provide 45 MW of area-1 power based on their participation factors, while Genco G2 provides 5 MW through a bilateral contract. Figure 11 depicts changes in the power output of area-1.
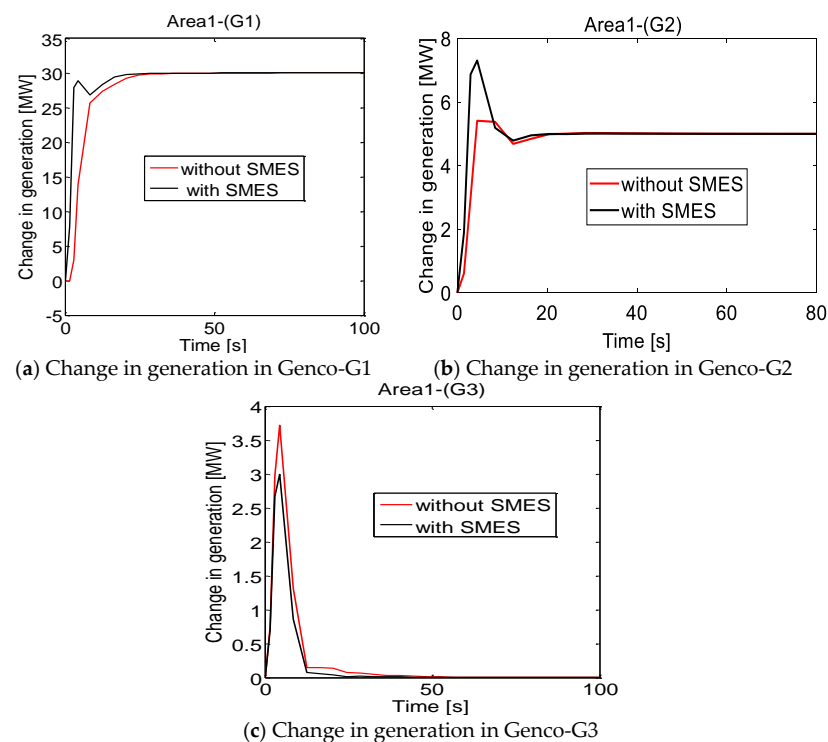

(**a**) Change in generation in Genco-G1   (**b**) Change in generation in Genco-G2

(**c**) Change in generation in Genco-G3

Figure 11. Change in Gencos in area-1 (MW).

In area-2: Area-2 encounters a total load demand of 50 MW. Gencos with bilateral and Poolco transactions participate and manage their generation to meet this demand. G4 and G5 are involved in the bilateral transaction. G6 and G8 are involved in Poolco. To meet bilateral transactions of area-2, G4 reduces its effective power by 5 MW. G5 increases its output by 15 MW to meet 10% of area-1 load and 10% of area-4 load. Bilateral transactions provide 30% of the demand for area-2 load. As a result, G6 and G8 split the remaining demand (35 MW) according to their participation parameters. G6 changes to 5 W and G8 to 25 MW. The load on D6 is reduced by 5 MW. The change in the generation is shown in Figure 12.
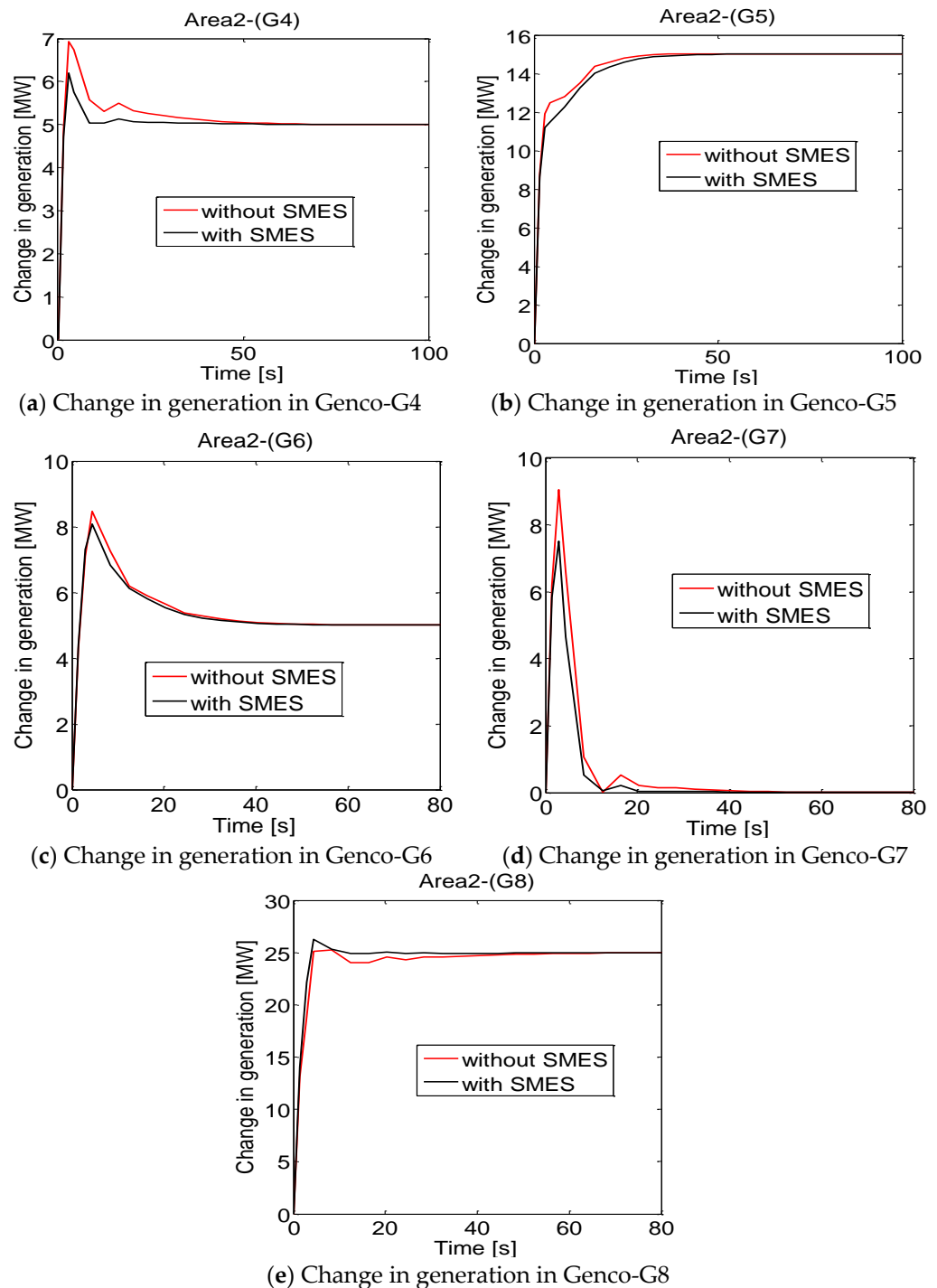
(**a**) Change in generation in Genco-G4

(**b**) Change in generation in Genco-G5

(**c**) Change in generation in Genco-G6

(**d**) Change in generation in Genco-G7

(**e**) Change in generation in Genco-G8

Figure 12. Change in Gencos in area-2 (MW).

In area-3: Due to the absence of bilateral transaction, for better performance G9 and G10 participate to meet the load requirement of area-3. G9 regulates 15 MW of real power and G10 increases up to 35 MW. Figure 13 depicts changes in the real power output of area-3 in Gencos.
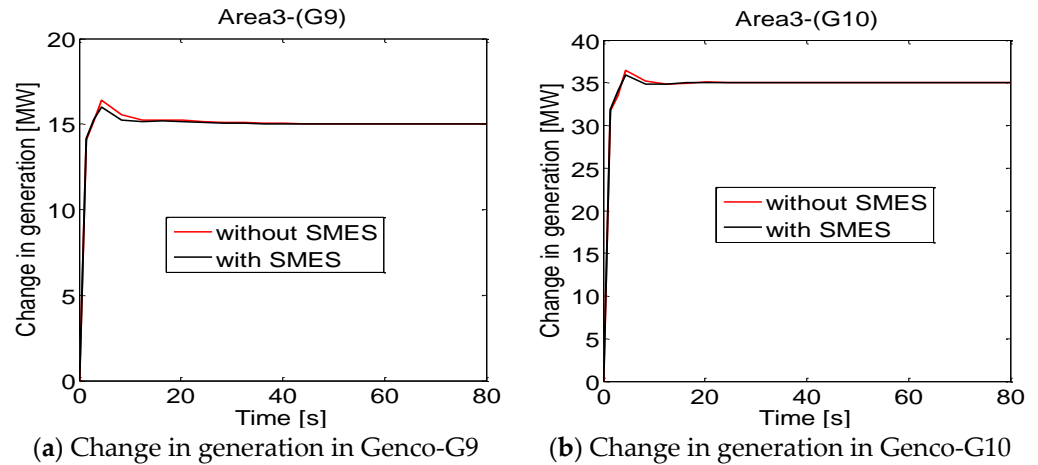

(**a**) Change in generation in Genco-G9   (**b**) Change in generation in Genco-G10

Figure 13. Change in Gencos in area-3 (MW).

In area-4: Genco G11 supplies 20% of 2-area load demand of 50 MW. Through bilateral transaction, 30% of the load demand of area-4 is provided. G12 (area-4) changes its generation to supply 20% of area-4 load. A total of 10% of area-4 load is supplied by G5 (area-2). The demand of 70 MW is to be fulfilled by Gencos G11, G13, G15 and D11 of area-4. G11 considers 20% of area-2 load demand. G12 of area-4 modifies by 20 MW to supply 20% of area-4 load, and G5 of area-2 supplies 10% of area-4 load through bilateral exchanges. G11 regulates its power by 25 MW, G13 by 10 MW and G15 by 25 MW. D1 lowers its load by 10 MW. Figure 14 depicts the changes in Gencos of area-4.
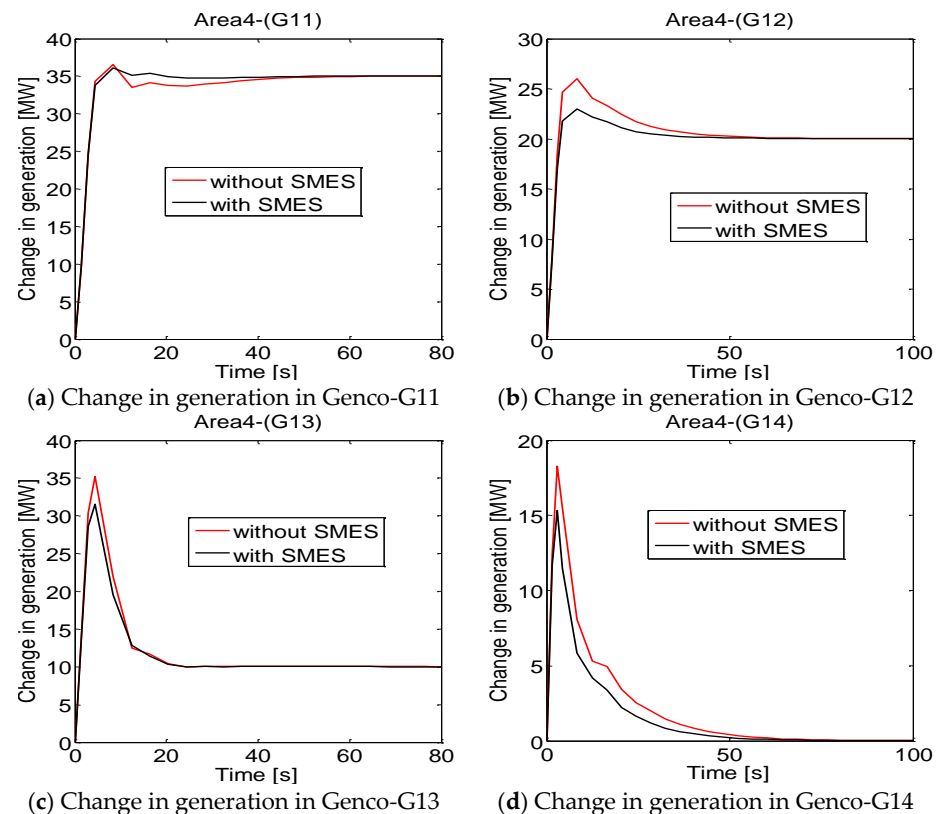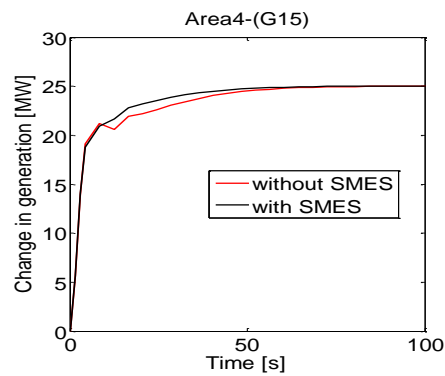

(**a**) Change in generation in Genco-G11   (**b**) Change in generation in Genco-G12

(**c**) Change in generation in Genco-G13   (**d**) Change in generation in Genco-G14

Figure 14. *Cont.*

(**e**) Change in generation in Genco-G15

Figure 14. Change in Gencos in area-4 (MW).

Figure 15 demonstrates that due to bilateral transactions, 5 MW of power is transmitted from area-2 to area-1, while it settles to zero in area-3 and area-4.
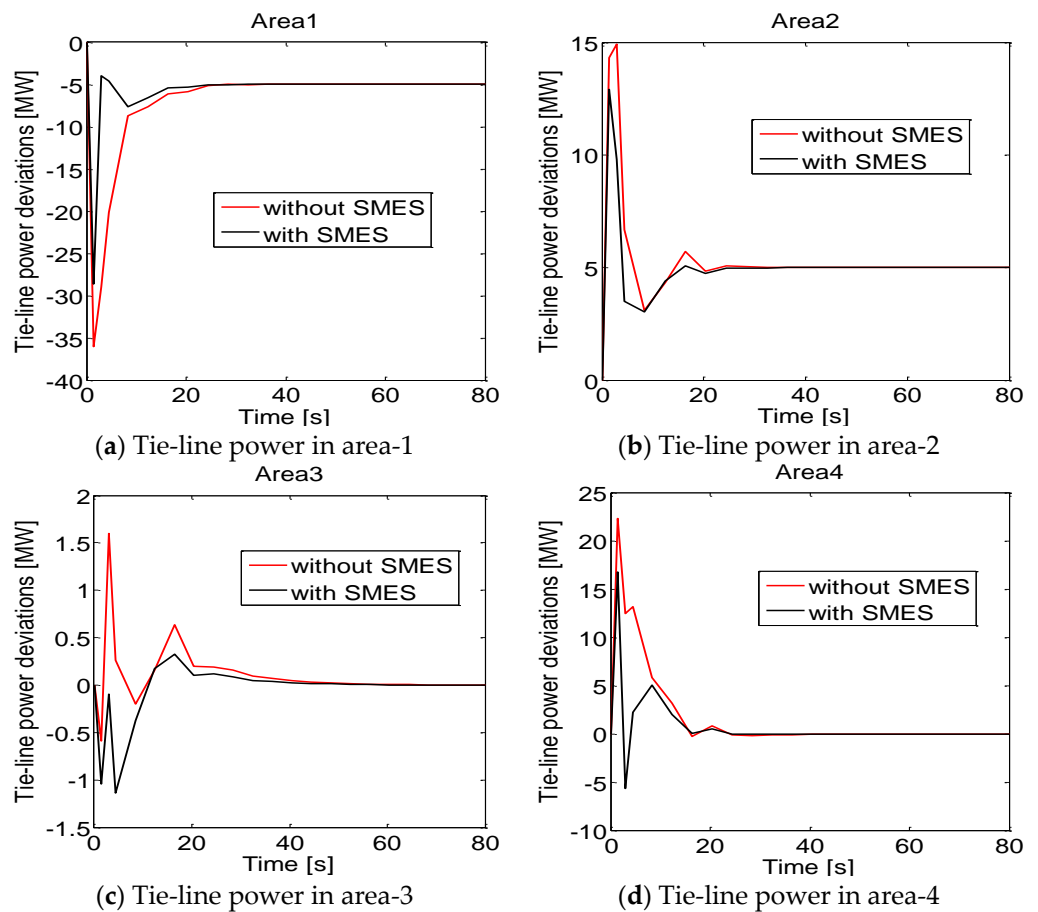

(**a**) Tie-line power in area-1

(**b**) Tie-line power in area-2

(**c**) Tie-line power in area-3

(**d**) Tie-line power in area-4

Figure 15. Tie-line power flow in all areas (MW).

As shown in Figure 16, the frequency of different areas settled faster to its target value using the SMES unit.
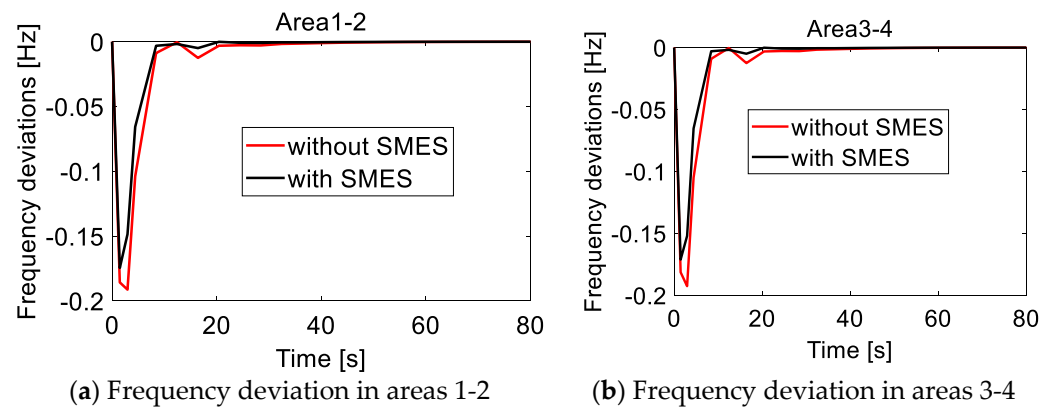
(**a**) Frequency deviation in areas 1-2

(**b**) Frequency deviation in areas 3-4

Figure 16. Frequency settlement in all areas (Hz).

The curtailment in Discos (D1, D2, D4) is shown in Figure 17, respectively.

(**a**) Change in demand of Discos in areas 1 & 4
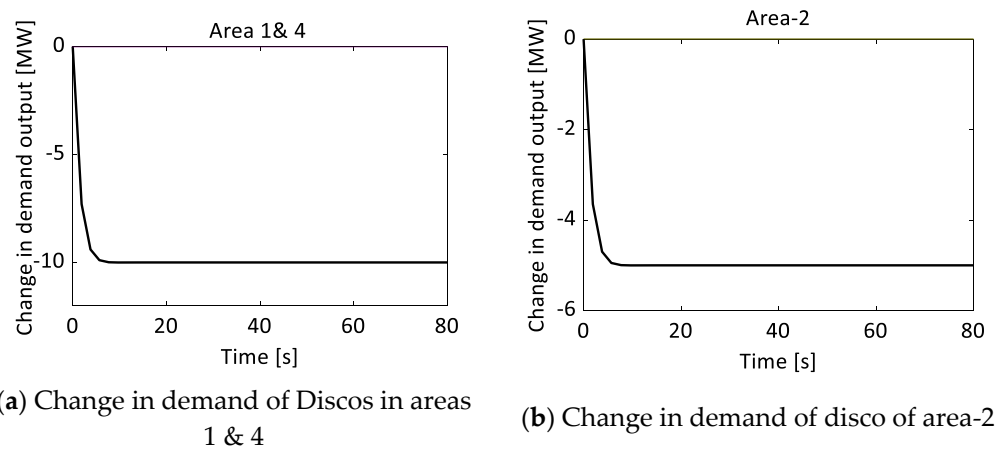

(**b**) Change in demand of disco of area-2

Figure 17. Change in load in areas-1,2,4 (MW).

Table 5 shows the type of contracts for different Gencos/Discos. Table 6 compares the performance of FOPID controllers with and without the SMES unit in terms of maximum overshoot/undershoot and settling time of area-1 and area-4 frequency deviations. Table 7 shows the parameters for FOPID controllers with SMES unit.

Table 5. Power transactions in different control areas.

Areas	Bilateral	Poolco
Area-1	G5	G2, D1, G1
Area-2	G11, G4	G8, D5, G4 G6
Area-3	none	G10, G9
Area-4	G5, G12	G11, G15, D11, G12 G13

Table 6. Analysis for frequency deviations.

Controller	Max. Undershoot (Area-1)	Max. Overshoot (Area-1)	Settling Time (s)
SMES	−0.175	0.0	45
No SMES	−0.19	0.00	60
Controller	Max. undershoot (Area-4)	Max. overshoot (Area-4)	Settling time (s)
SMES	−0.168	0.0	45
No SMES	−0.195	0.0	65

Table 7. Optimum values for FOPID control scheme.

	2-Area				
	K$_P$	**K$_I$**	**K$_D$**	λ	μ
	−0.997	**−0.985**	**−0.97**	**1.8**	**1.4**
	4-Area				
	K$_P$	**K$_I$**	**K$_D$**	λ	μ
Area-1	−1.781	−1.578	2.984	1.155	0.047
Area-2	−5.746	−1.287	−1.534	0.98	1.168
Area-3	−9.935	−2.957	−6.203	0.514	1.466
Area-4	−0.42	−1.363	0.326	1.484	1.578

5. Discussion

From the results obtained for two area and four area power systems, it is evident that the performance of an FOPID control scheme is improved in the presence of an SMES device, in terms of settling time and oscillations. The SMES device dampens the system quickly and helps to minimize deviations in the minimum time as given in various tables.

6. Conclusions

In this paper, a frequency-related issue in the presence of SMES units in a restructured multi-area power system is investigated. Two area and four area power systems incorporating bilateral and Poolco transactions are employed to simulate different cases to check the performance of the designed control scheme. A FOPID control scheme optimally tuned using BBBC is utilized in this paper. It is evident that the FOPID control scheme gives better results and improves its performance in the presence of an SMES unit. The SMES helps to dampen the response quickly when a sudden load disturbance occurs. At steady state, the frequency error is seen to be zero in all circumstances. Furthermore, the simulation confirms that the proposed control scheme is successful and produces better outcomes, such as shorter settling times, less overshoot and faster damping, because the FOPID controller performs better in the presence of an SMES unit.

Nomenclature

LFC	Load frequency control
AGC	Automatic generation control
FOPID	Fractional order proportional integral derivative
BBBC	Big Bang Big Crunch
PSO	Particle swarm optimization
Ptie	Tie-line power
ICA	Imperialistic competition algorithm
PID	Proportional Integral Derivative
DPM	Disco Participation Matrix
ACE	Area control error

References

1. Elgerd, O.I.; Fosha, C. Optimum megawatt- frequency control of multi-area electric energy systems. *IEEE Trans. Power Syst.* **1970**, *89*, 556–563. [CrossRef]
2. Christie, R.D.; Bose, A. Load frequency control issues in power system operation after deregulation. *IEEE Trans. Power Syst.* **1996**, *11*, 1191–1200. [CrossRef]
3. Pandey, S.K.; Mohanty, S.R.; Kishor, N. A literature survey on load–frequency control for conventional and distribution generation power systems. *Renew. Sustain. Energy Rev.* **2013**, *25*, 318–334. [CrossRef]
4. Tan, W. Tuning of PID load frequency controller for power systems. *Energy Convers. Manag.* **2009**, *50*, 1465–1472. [CrossRef]
5. Shayeghi, H.; Jalili, A.; Shayanfar, H.A. A robust mixed H2/H∞ based LFC of a deregulated power system including SMES. *Energy Convers. Manag.* **2008**, *49*, 2656–2668. [CrossRef]
6. Pappachen, A.; Fathima, A.P. Load frequency control in deregulated power system integrated with SMES–TCPS combination using ANFIS controller. *Int. J. Electr. Power Energy Syst.* **2016**, *82*, 519–534. [CrossRef]
7. Changmao, Q.; Naiming, Q.; Zhiguo, S. Fractional PID controller design of hypersonic flight vehicle, computer, mechatronics. In Proceedings of the 2010 IEEE International Conference on Computer, Mechatronics, Control and Electronic Engineering (CMCE), Changchun, China, 24–26 August 2010; pp. 466–469.
8. Hamamci, S.E. An algorithm for stabilization of fractional-order time delay systems using fractional-order PID controllers. *IEEE Trans. Autom. Control* **2007**, *52*, 1964–1969. [CrossRef]
9. Zamani, M.; Ghartemani, M.K.; Sadati, N.; Parniani, M. Design of fractional order PID controller for an AVR using particle swarm optimization. *Control Eng. Pract.* **2009**, *17*, 1380–1387. [CrossRef]
10. Yang, F.; Shao, X.; Muyeen, S.M.; Li, D.; Lin, S.; Fang, C. Disturbance Observer based Fractional-order Integral Sliding Mode Frequency Control Strategy for Interconnected Power System. *IEEE Trans. Power Syst.* **2021**, *36*, 5922–5932. [CrossRef]
11. Oshnoei, S.; Oshnoei, A.; Mosallanejad, A.; Haghjoo, F. Contribution of GCSC to regulate the frequency in multi-area power systems considering time delays: A new control outline based on fractional order controllers. *Int. J. Electr. Power Energy Syst.* **2020**, *123*, 106197. [CrossRef]
12. Debbarma, S.; Saikia, L.C.; Sinha, N. AGC of a multi–area thermal system under deregulated enviornment using a non–integer controller. *Electr. Power Syst. Res.* **2013**, *95*, 175–183. [CrossRef]
13. Erol, O.K.; Eskin, I. New optimization method: Big bang–big crunch. *Adv. Eng. Softw.* **2006**, *37*, 106–111. [CrossRef]
14. Kumar, N.; Tyagi, B.; Kumar, V. Multi-area deregulated automatic generation control scheme of power system using imperialist competitive algorithm based robust controller. *IETE J. Resea.* **2017**, *64*, 528–537. [CrossRef]
15. Kumar, N.; Tyagi, B.; Kumar, V. Multi Area AGC scheme using Imperialist Competition Algorithm in Restructured Power System. *Appl. Soft Comput.* **2016**, *48*, 160–168. [CrossRef]
16. Kumar, N.; Tyagi, B.; Kumar, V. Deregulated multiarea AGC scheme using BBBC-FOPID controller. *Arab. J. Sci. Eng.* **2016**, *42*, 2641–2649. [CrossRef]
17. Kumar, N.; Malik, H.; Singh, A.; Alotaibi, M.A.; Nassar, M.E. Novel Neural Network-Based Load Frequency Control Scheme: A Case Study of Restructured Power System. *IEEE Access* **2021**, *9*, 162231–162242. [CrossRef]
18. Mahto, T.; Malik, H.; Bin Arif, M.S. Load Frequency Control of A Solar-Diesel Based Isolated Hybrid Power System By Fractional Order Control Using Particle Swarm Optimization. *J. Intell. Fuzzy Syst.* **2018**, *35*, 5055–5061. [CrossRef]
19. Mahto, T.; Kumar, R.; Malik, H.; Hussain, S.; Ustun, T. Fractional Order Fuzzy based Virtual Inertia Controller Design for Frequency Stability in Isolated Hybrid Power Systems. accepted for publication. *Energies* **2021**, *14*, 1634. [CrossRef]
20. Mahto, T.; Malik, H.; Mukherjee, V.; Alotaibi, M.A.; Almutairi, A. Renewable Generation Based Hybrid Power System Control Using Fractional Order-Fuzzy Controller. *Energy Rep.* **2021**, *7*, 641–653. [CrossRef]